C. R. Chimie 20 (2017) 934–941

Contents lists available at ScienceDirect

Comptes Rendus Chimie

www.sciencedirect.com

Full paper/Mémoire

A mild and convenient protocol for the conversion of toxic acid red 37 into pharmacological (antibiotic and anticancer) nominees: Organopalladium architectures

Reda F.M. Elshaarawy [a, b, *], Tahany M. Sayed [c], Haniya M. Khalifa [c], Emtithal A. El-Sawi [c, **]

[a] Institut für Anorganische Chemie und Strukturchemie, Heinrich-Heine Universität Düsseldorf, 40204 Düsseldorf, Germany
[b] Chemistry Department, Faculty of Science, Suez University, 43518 Suez, Egypt
[c] Department of Chemistry, Faculty of Women for Arts, Science and Education, Ain Shams University, Heliopolis, Cairo, Egypt

ARTICLE INFO

Article history:
Received 31 May 2017
Accepted 13 July 2017
Available online 18 August 2017

Keywords:
Anticancer
Antimicrobial
Acid red 37
Schiff base
Organopalladium

ABSTRACT

Diverse applications of azo dyes in textiles, paper, leather, cosmetics, pharmaceutical, and food industries along with their deleterious impacts on human beings and aquatic life have raised urgent calls for the treatment of effluent containing azo dyes to remove them or convert them into useful and safe products. This inspires us to modulate acid red 37 to acid red Schiff bases (ARSBs), which were further palladinated to yield monopalladated products (Pd(II)-ARSBs) with an emphasis to obtain new pharmacological (antibiotic and anticancer) candidates. These new cyclopalladated complexes were structurally characterized and pharmacologically evaluated as well for their in vitro antimicrobial, against a common panel of pathogenic G^+ and G^- bacterial and fungal strains, and anticancer activities against human breast carcinoma (MCF-7) cell lines.

1. Introduction

Synthetic dyes, such as acid red 37 (AR-37) and azo dyes, are widely used in the textile, leather, polyamide fiber, cosmetics, and food industries [1]; however, their toxicity, carcinogenic, or genotoxic effects on the environment and humans [2] remain the major drawbacks and limited their wide applications. Moreover, removal of these dyes from the industrial effluents or converting them into useful byproducts before discharge is a great environmental challenge for safe industries [3]. Conventional physico-chemical methods including adsorption, floatation, coagulation, incineration, neutralization, reduction, oxidation, electrolysis, and ion-exchange of these dyes are quite expensive, inapplicable for a wide variety of dyes, and may produce a lot of more toxic sludge and byproducts [4]. Therefore, identification of a novel strategy to detoxify these synthetic dyes is of great interest. Motivated by our interest in the development of new pharmacologically relevant architectures for pharmaceutical applications [5,6], we aimed herein to apply subsequent Schiff-base (SB) condensation and palladination strategies for conversion of AR-37 into pharmacologically useful active products.

Our choice for SBs and their organopalladium complexes as target products is because of their unrivaled features such as simplicity of the preparation, remarkable flexibility of their molecular and electronic structure, and their wide range of pharmacological activities including antibacterial, antifungal, antimalarial, antitubercular, anti-proliferative, anti-inflammatory, and antiviral [7]. Furthermore, many reported azomethine Pd(II) chelates exhibited

* Corresponding author.
** Corresponding author.
E-mail addresses: reel-001@uni-duesseldorf.de, reda.elshaarawi@science.suez.edu.eg (R.F.M. Elshaarawy), elsawi_e@yahoo.com (E.A. El-Sawi).

http://dx.doi.org/10.1016/j.crci.2017.07.003
1631-0748/

significant promising antiviral, fungicidal, bactericidal, and antitumor activities [8]. Moreover, palladium plays a crucial role in the metallotherapeutic drugs and metal-based diagnostic agents [8]. For example, anticancer screening for organopalladium of acetone SBs that bear *S*-methyldithiocarbazate and *S*-benzyldithiocarbazate compartments against T-lymphoblastic leukemia cell lines demonstrated excellent cytotoxicity in comparison to the standard anticancer drug, tamoxifen [9].

Inspired by the aforementioned literature outputs and in continuation of our endeavor directed toward designing and development of novel biologically potent materials, we planned herein to apply SB condensation and palladination chemistries for conversion of toxic AR-37 into beneficial pharmacologically (antimicrobial and anticancer) active acid red Schiff bases (ARSBs) and *endo*-cyclic five/six-membered cyclopalladated complexes.

2. Experimental section

2.1. Reagents and materials

Chemicals were obtained from the following suppliers and used without further purification: AR-37, 4-chlorobenzaldehyde, 4-methoxybenzaldehyde, anthracen-9(10*H*)-one, 4-nitrobenzaldehyde, and anthracene-9-carbaldehyde (Sigma–Aldrich) and palladium(II) chloride ($PdCl_2$) (Acros).

2.2. Instrumentation

Melting points were measured using a Gallenkamp melting point apparatus; all melting points were measured in open glass capillaries and are uncorrected. Thin layer chromatography was performed with fluorescent silica gel plates HF254 (Merck), and plates were viewed under ultraviolet light at 254 and 265 nm. The elemental analyses for C, H, and N were determined by a Perkin–Elmer Analyzer 2440. Fourier transform infrared (FTIR) spectra were recorded on a Bruker Vector Germany and on a Mattson FTIR spectrophotometer in the range of 400–4000 cm^{-1} as KBr disc with 2 cm^{-1} resolution. For signal intensities the following abbreviations were used: br (broad), sh (sharp), w (weak), m (medium), s (strong), vs (very strong). ^1H NMR spectra were recorded on a Gemini 200 MHz spectrometer, in dimethyl sulfoxide (DMSO)-d_6 solution with calibration to the residual proton solvent signal in DMSO-d_6 (^1H NMR: 2.52 ppm) against tetramethylsilane (TMS) ($\delta = 0.00$ ppm). Multiplicities of the signals were specified as s (singlet), d (doublet), t (triplet), q (quartet), or m (multiplet). The mass spectra of the synthesized compounds were measured on GCQ Finnigan MAT. For the mass spectral assignment, peaks are based on ^{12}C with 12.0000 Da.

2.3. Solvent-free microwave-assisted synthesis of ligands (ARSB**1**–**6**)

AR-37 SB ligands were synthesized according to the literature procedure [10] assisted with microwave irradiation. Generally, in a microwave flask, the AR-37 (0.25 mmol) and appropriate aromatic aldehydes (0.50 mmol) were introduced and homogenized. The mixture was submitted to microwave irradiation at ambient pressure for 15 min at 200 W (150 °C) without the solvent. The crude product was cooled, washed with CH_2Cl_2 (5 mL), and crystallized from the suitable solvent. The pure product was filtered off under reduced pressure. The details for the physical, elemental analysis, and spectral data of all ligands (ARSB**1**–**6**) are provided in our previous work [10].

2.4. Synthesis of organopalladium complexes (Pd(II)-ARSBs)

Generally, 1 mmol of the parent ligand (ARSB**1**–**6**) was added to an ethanolic solution (60 mL) of palladium(II) chloride (1 mmol) containing few drops of concentrated HCl. Then, the mixture was stirred for 4 h under reflux and nitrogen atmosphere, the isolated product was filtered off, washed with cold ethanol (5 mL ×3), ether (5 mL ×3), and finally dried under vacuum. Further crystallization from the methanol affords pure complexes (Pd(II)-ARSBs). Samples of isolated organopalladium complexes were characterized as follow.

[Pd(ARSB**1**)Cl] (Pd-ARSB**1**): Obtained as orange crystals in 80.5% yield; mp = 330 °C. FTIR (KBr, cm^{-1}): 3405 (s, br, $\nu_{(O-H)}$), 3065 (m, sh, $\nu_{asym(C-H)}$, Ar), 3040 (m, sh, $\nu_{sym(C-H)}$, Ar), 2940 (s, br, $\nu_{(C-H)}$), 1644 (s, sh, $\nu_{(C=O)}$), 1599 (s, sh, $\nu_{(C=N)}$, azomethine), 1497, 1421 (s, sh, $\nu_{(C=C_{Ar}+C-H_{bend})}$), 575 (m, sh, $\nu_{(C-Pd)}$). ^1H NMR (200 MHz, DMSO-d_6) δ (ppm): 12.28 (s, 1H), 10.20 (s, 1H), 8.10 (S, 1H), 7.83 (d, $J = 6.8$ Hz, 1H), 7.78–7.65 (m, 5H), 7.59 (s, 1H), 7.45–7.33 (m, 3H), 7.30–7.19 (m, 2H), 7.11–6.98 (m, 3H), 2.50 (s, br, 2H), 2.02 (s, 2H). EI-MS: *m*/*z* (intensity) 883.50 (31.05%) ($C_{32}H_{21}Cl_3N_4O_8PdS_2$ $[M]^{+\bullet}$). Anal. Calcd (%) for $C_{33}H_{21}Cl_3N_4O_8PdS_2$ (M = 866.44 g/mol): C, 44.36; H, 2.44; N, 6.47; S, 7.40. Found (%): C, 44.28; H, 2.56; N, 6.32; S, 7.11.

[Pd(ARSB**2**)Cl] (Pd-ARSB**2**): Obtained as red crystals in 85.5% yield; mp = 327 °C. FTIR (KBr, cm^{-1}): 3435 (s, br, $\nu_{(O-H)}$), 3195 (s, br, $\nu_{(N-H)}$), 3065 (m, sh, $\nu_{asym(C-H)}$, Ar), 3040 (m, sh, $\nu_{sym(C-H)}$, Ar), 2608 (s, br, $\nu_{(C-H)}$), 1644 (s, sh, $\nu_{(C=O)}$), 1598 (s, sh, $\nu_{(C=N)}$, azomethine), 1497, 1393 (s, sh, $\nu_{(C=C_{Ar}+C-H_{bend})}$), 575 (m, sh, $\nu_{(C-Pd)}$). ^1H NMR (200 MHz, DMSO-d_6) δ (ppm): 12.33 (s, 1H), 10.28 (s, 1H), 8.56 (s, 1H), 8.21 (d, $J = 7.1$ Hz, 1H), 7.92 (d, $J = 6.9$ Hz, 2H), 7.79–7.68 (m, 3H), 7.51 (d, $J = 7.2$ Hz, 1H), 7.44 (d, $J = 1.8$ Hz, 1H), 7.38–7.21 (m, 2H), 7.15–7.03 (m, 3H), 3.97 (s, 3H), 3.90 (s, 3H), 2.53 (s, br, 2H). EI-MS: *m*/*z* (intensity) 857.50 (5.06%) ($C_{34}H_{27}ClN_4O_{10}PdS_2$ $[M]^{+\bullet}$). Anal. Calcd (%) for $C_{34}H_{27}ClN_4O_{10}PdS_2$ (M = 857.50 g/mol): C, 47.62; H, 3.17; N, 6.53; S, 7.48. Found (%): C, 47.58; H, 3.25; N, 6.43; S, 7.31.

[Pd(ARSB**3**)Cl] (Pd-ARSB**3**): Obtained as brown crystals in 85.3% yield; mp = 319 °C. FTIR (KBr, cm^{-1}): 3397 (s, br, $\nu_{(O-H)}$), 3299 (s, sh, NH), 3062 (m, sh, $\nu_{asym(C-H)}$, Ar), 3025 (m, sh, $\nu_{sym(C-H)}$, Ar), 2927 (s, br, $\nu_{(C-H)}$), 1658 (s, sh, $\nu_{(C=O)}$), 1595 (s, sh, $\nu_{(C=N)}$, azomethine), 1458, 1403 (s, sh, $\nu_{(C=C_{Ar}+C-H_{bend})}$), 572 (m, sh, $\nu_{(C-Pd)}$). ^1H NMR (200 MHz, DMSO-d_6) δ (ppm): 11.98 (s, 1H), 10.28 (s, 1H), 8.45 (s, 1H), 8.13 (d, $J = 7.3$ Hz, 1H), 7.96–7.78 (m, 5H), 7.63–7.49 (m, 4H), 7.37–7.25 (m, 4H), 7.21–7.07 (m, 4H), 6.96 (d, $J = 1.8$ Hz, 1H), 2.61 (s, br, 2H). EI-MS: *m*/*z* (intensity) 956 (0.56%) ($C_{46}H_{30}ClN_4O_7PdS_2$ $[M-OH]^{+\bullet}$). Anal. Calcd (%) for $C_{46}H_{31}ClN_4O_8PdS_2$ (M = 973.76 g/mol): C, 56.74; H, 3.21; N, 5.75; S, 6.59. Found (%): C, 56.50; H, 3.25; N, 5.54; S, 6.50.

[Pd(ARSB**4**)(CH_3OH)(H_2O)] (Pd-ARSB**4**): Obtained as brown crystals in 86.0% yield; mp = 341 °C. FTIR (KBr, cm^{-1}): 3436 (s, br, $\nu_{(O-H)}$), 3066 (m, sh, $\nu_{asym(C-H)}$, Ar), 2923 (s, br, $\nu_{(C-H)}$), 1697 (s, sh, $\nu_{(C=O)}$), 1626 (s, sh, $\nu_{(C=N)}$, azomethine), 1525, 1349 (m, sh, NO_2), 1494, 1441 (s, sh, $\nu_{(C=C_{Ar}+C-H_{bend})}$), 575 (m, sh, $\nu_{(C-Pd)}$). ^{1}H NMR (200 MHz, DMSO-d_6) δ (ppm): 11.67 (s, 1H), 8.71 (s, 1H), 8.53–8.34 (m, 5H), 8.12–8.01 (m, 3H), 7.77 (d, J = 7.3 Hz, 2H), 7.65 (d, J = 7.0 Hz, 1H), 7.37–7.28 (m, 2H), 2.51 (s, br, 2H), 2.23 (s, 3H), 1.18 (s, 3H). EI-MS: m/z (intensity) 869 (1.03%) ($C_{32}H_{22}N_6O_{13}PdS_2$ $[M-CH_3OH-H_2O]^{+\bullet}$). Anal. Calcd (%) for $C_{33}H_{28}N_6O_{15}PdS_2$ (M = 919.16 g/mol) C, 43.12; H, 3.07; N, 9.14; S, 6.98. Found (%): C, 43.00; H, 3.00; N, 9.20; S, 6.90.

[Pd(ARSB**5**)(CH_3OH)(H_2O)] (Pd-ARSB**5**): Obtained as orange crystals in 84.0% yield; mp = 325 °C. FTIR (KBr, cm^{-1}): 3432 (s, br, $\nu_{(O-H)}$), 3073 (m, sh, $\nu_{asym(C-H)}$, Ar), 2925 (s, br, $\nu_{(C-H)}$), 1664 (s, sh, $\nu_{(C=O)}$), 1623 (s, sh, $\nu_{(C=N)}$, azomethine), 1487, 1445 (s, sh, $\nu_{(C=C_{Ar}+C-H_{bend})}$), 578 (m, sh, $\nu_{(C-Pd)}$), 528 (m, sh, $\nu_{(O-Pd)}$). ^{1}H NMR (200 MHz, DMSO-d_6) δ (ppm): 11.98 (s, 1H), 8.75 (s, 1H), 8.58–8.43 (m, 4H), 8.10–7.96 (m, 4H), 7.78–7.63 (m, 5H), 7.59 (d, J = 7.0 Hz, 2H), 7.55 (d, J = 7.1 Hz, 2H), 7.51 (t, $J_1 = J_2$ = 7.2 Hz, 2H), 7.48 (d, J = 7.3 Hz, 2H), 7.39–7.25 (m, 5H), 2.51 (s, br, 2H), 2.26 (s, 3H), 1.22 (s, 3H). EI-MS: m/z (intensity) 979 (13.93%) ($C_{48}H_{32}N_4O_9PdS_2$ $[M-CH_3OH-H_2O]^{+\bullet}$). Anal. Calcd (%) for $C_{49}H_{38}N_4O_{11}PdS_2$ (M = 1029.40 g/mol) C, 57.17; H, 3.72; N, 5.44; S, 6.23. Found (%): C, 57.00; H, 3.82; N, 5.30; S, 6.20.

[Pd(ARSB**6**)($CH_3OH)_2$]H_2O (Pd-ARSB**6**): Obtained as red crystals in 88.0% yield; mp = 337 °C. FTIR (KBr, cm^{-1}): 3438 (s, br, $\nu_{(O-H)}$), 3076 (m, sh, $\nu_{asym(C-H)}$, Ar), 2931 (s, br, $\nu_{(C-H)}$), 1658 (s, sh, $\nu_{(C=O)}$), 1625 (s, sh, $\nu_{(C=N)}$, azomethine), 1485, 1448 (s, sh, $\nu_{(C=C_{Ar}+C-H_{bend})}$), 580 (m, sh, $\nu_{(C-Pd)}$), 529 (m, sh, $\nu_{(O-Pd)}$). ^{1}H NMR (200 MHz, DMSO-d_6) δ (ppm): 12.27 (s, 1H), 8.78 (s, 1H), 8.61–8.49 (m, 3H), 7.87–7.70 (m, 5H), 7.61–7.51 (m, 2H), 7.22 (d, J = 7.0 Hz, 2H), 7.13 (d, J = 6.9 Hz, 2H), 7.01 (t, $J_1 = J_2$ = 7.1 Hz, 2H), 6.88–6.76 (m, 3H), 3.37 (s, 3H), 3.28 (s, 3H), 3.19 (s, 3H), 2.48 (s, br, 2H), 2.35 (s, 2H), 1.16 (s, 6H). EI-MS: m/z (intensity) 1077 (5.52%) ($C_{47}H_{52}N_7O_{12}PdS_2$ $[M-H]^+$). Anal. Calcd (%) for $C_{47}H_{53}N_7O_{12}PdS_2$ (M = 1078.51 g/mol) C, 52.34; H, 4.95; N, 9.09; S, 5.95. Found (%): C, 52.25; H, 4.80; N, 9.00; S, 5.92.

3. Pharmacological studies

3.1. Antimicrobial activity

3.1.1. Reagents

DMSO, tetracycline (Tetrcy) antibiotic ($C_{22}H_{24}N_2O_8$, 444,44 g mol^{-1}), and amphotericin B (Am B) ($C_{47}H_{73}NO_{17}$, 923.49 g mol^{-1}), antifungal drug were obtained from Sigma Chemical Co (St. Louis, MO).

3.1.2. Microbial cultures

Strains used in this study were from National Organization for Drug Control and Research, Cairo, Egypt. The different strains are *Staphylococcus aureus* (RCMB 010027) and *Streptococcus faecalis* as representatives for the G^+ bacteria, whereas *Escherichia coli* (RCMB 010059) and *Pseudomonas aeruginosa* as the most important G^- pathogenic bacteria. Antifungal species are *Aspergillus flavus* and *Candida albicans* (RCMB 05038). Stock cultures grown aerobically on nutrient broth agar slants (Hi-Media) at 37 °C were maintained at 4 °C. Precultures containing 105 CFU mL^{-1}, grown aerobically in Mueller Hinton liquid medium (Hi-Media) at 37 °C for 5 h, were used as inoculum for all experiments. Antimicrobial susceptibility of the microbial strains was carried out by agar well diffusion method [11] for the target compounds and standard drugs, Tetrcy, and Am B. The diameter of the zones of inhibition (ZOI, mm) was measured accurately as indicative of antimicrobial activity.

3.1.3. Determination of MIC

As parameters of the antibacterial efficacy, the minimal inhibitory concentrations (MICs) of the new compounds against infection isolates were determined using the macrodilution broth susceptibility test. Freshly prepared Mueller Hinton broth was used as diluent in the macrodilution method. A serial dilution of each compound was prepared within a desired range (0.25–20.00 mM). One milliliter of the stock cultures was then inoculated and tubes were incubated at 37 °C for 24 h, control tubes were assayed simultaneously. MIC was examined visually by checking the turbidity of the tubes.

3.2. In vitro anticancer activity

3.2.1. Cell cultures

Human breast carcinoma (MCF-7) cell lines were obtained from the American type culture collection (Rockville, MD). The cells were grown on RPMI-1640 medium supplemented with 10% inactivated fetal calf serum and 50 mg/mL gentamicin. The cells were maintained at 37 °C in a humidified atmosphere with 5% CO_2 and were subcultured two to three times a week.

3.2.2. Antitumor assay

The antitumor activity of new organopalladium complexes was evaluated against MCF-7 cell lines. The cancer cells were grown as monolayers in growth RPMI-1640 medium supplemented with 10% inactivated fetal calf serum and 50 mg/mL gentamicin. The monolayers of 104 cells adhered at the bottom of the wells in 69-well microtiter plates were incubated for 24 h at 37 °C in a humidified incubator with 5% CO_2. Fresh medium containing different concentrations of the tested sample in DMSO was added after 24 h of seeding. The monolayers were then washed with sterile phosphate-buffered saline (0.01 M, pH 7.2) with simultaneous treatment of the cells with 100 mL from different dilutions of a tested sample in a fresh maintenance medium and incubated at 37 °C for 48 h. A control of untreated cells was cultured in the absence of a tested sample. A positive control containing doxorubicin (Dox) drug was used for comparison. Six wells were used for each concentration of the examined sample. Every 24 h the observation under the inverted microscope was carried out. The number of the surviving cells was determined by staining the cells with sulforhodamine B stain [12], followed by cell lysing using 33% glacial acetic acid and then recording the absorbance at 590 nm using enzyme-linked immunosorbent assay (ELISA) reader (SunRise, TECAN, Inc,) after well mixing. The absorbance values collected from

untreated cells were considered as 100% proliferation. The number of viable cells was determined using ELISA reader as previously mentioned, and the percentage of viability was calculated as $\{(1 - (ODt/ODc)) \times 100\}$, where ODt is the mean optical density of wells treated with the tested sample and ODc is the mean optical density of untreated cells. The 50% inhibitory concentration (IC_{50}), the concentration required to cause toxic effect in 50% of intact cells, was estimated from graphic plots.

4. Results and discussion

4.1. Chemistry protocol

Microwave irradiation was used to induce a facile simultaneous dual functionalization (chalcone and SB) in AR-37 with aromatic aldehydes (*p*-chlorobenzaldehyde and *p*-methoxybenzaldehyde or anthrone) for preparation of a series new chalcone-functionalized ARSB**1**–**3**, which undergo further palladination with in situ prepared $H_2[PdCl_4]$ to give organopalladium complexes (Pd(II)-ARSB**1**–**3**) (see Scheme 1).

On the other hand, the electron-deficient aromatic aldehyde, *p*-nitrobenzaldehyde, or 9-anthracenecarbaldehyde reacts with AR-37 by nucleophilic addition along with SB condensation reactions under the same microwave conditions to yield new aminohydrin-functionalized ARSB**4**,**5**, which were palladinated with $H_2[PdCl_4]$ to give organopalladium complexes Pd(II)-ARSB**4**,**5** (see Scheme 2).

However, a highly electron-rich aromatic aldehyde, *p*-(*N*,*N*-dimethylamino)benzaldehyde (DMAB), reacts with AR-37 by an unexpected triple-reactions pathway (condensation, nucleophilic addition, and SB) to give bifunctional chalcone/aminohydrin-functionalized ARSB**6**, which was further palladinated with $H_2[PdCl_4]$ affording the corresponding organopalladium complex Pd(II)-ARSB**6** (see Scheme 3).

The structures of a new organopalladium compound were assigned based upon the microanalytical and spectral analysis (IR, ^{1}H NMR, and electron impact mass spectra [EI-MS]).

4.2. Characterizations of the organopalladium compounds

4.2.1. Microanalytical data and mass spectrometry

The new organopalladium compounds (Pd(II)-ARSB**1**–**6**) were prepared in convinced yields, and their microanalytical data (C, H, N, and S analyses) are in good agreement with our proposed structural formulas (see Section 2).

The EI-MS of new organopalladium complexes are synonymous with their low stability as revealed by minimum contribution (0.56%–13.93%) of its molecular ion peak $[M]^{+\bullet}$, a molecular mass signature. This reduced stability led to a higher level of fragmentation along with enhanced contribution of produced fragments. The fragmentation pattern of Pd(II)-ARSB**5**, as a representative example for organopalladium complexes, is depicted in Scheme 4.

4.2.2. IR spectroscopic data

Emergence of new C–Pd vibrational band along with the remarkable shift in the native bands in the recorded FTIR spectra of organopalladium complexes as compared with those of parent ligands provides strong evidence for the successful palladination of ARSB**1**–**6** and simultaneously assigns the coordination sphere for each Pd(II) ion in its complexes. For instance, the two remarkable displacements of the azo (N=N) and phenolic (C–O) groups to a lower and higher frequencies by 22–29 and 12–21 cm^{-1}, respectively, in the spectra of Pd(II)-ARSB**1**–**3** confirm the

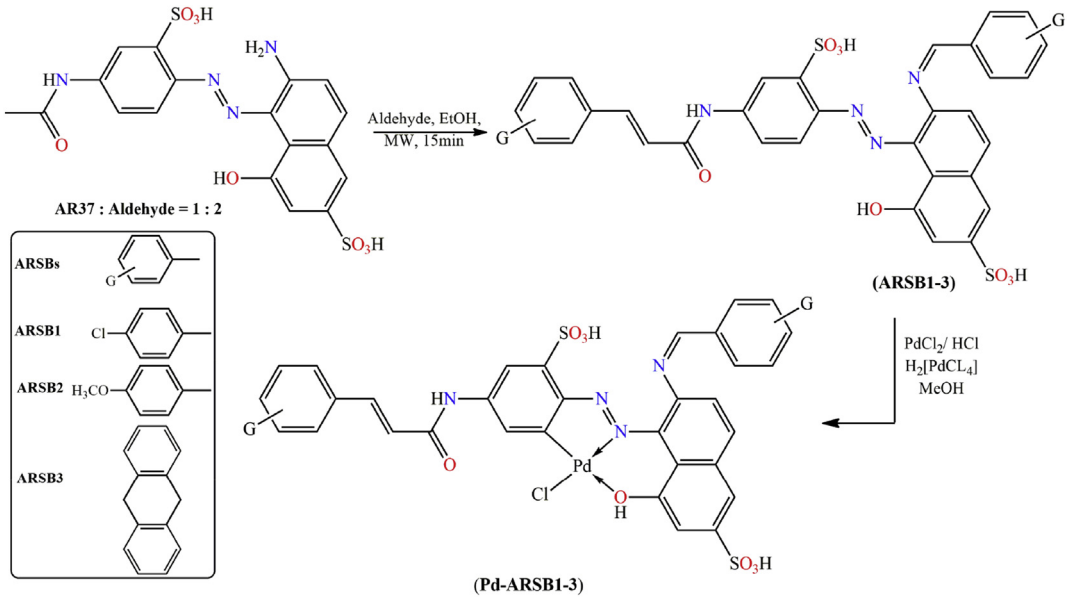

Scheme 1. Schematic diagram for the synthesis of ARSB**1**–**3** and their palladination to (Pd(II)-ARSB**1**–**3**).

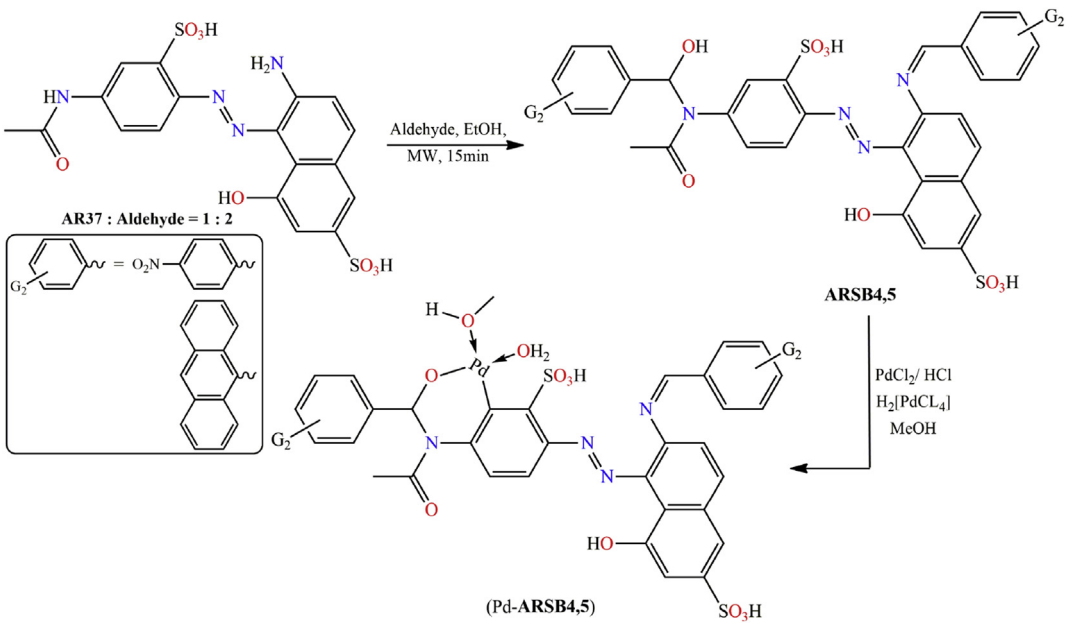

Scheme 2. Schematic preparation of ARSB**4**,**5** and their organopalladium compounds, (Pd(II)-ARSB**4**,**5**).

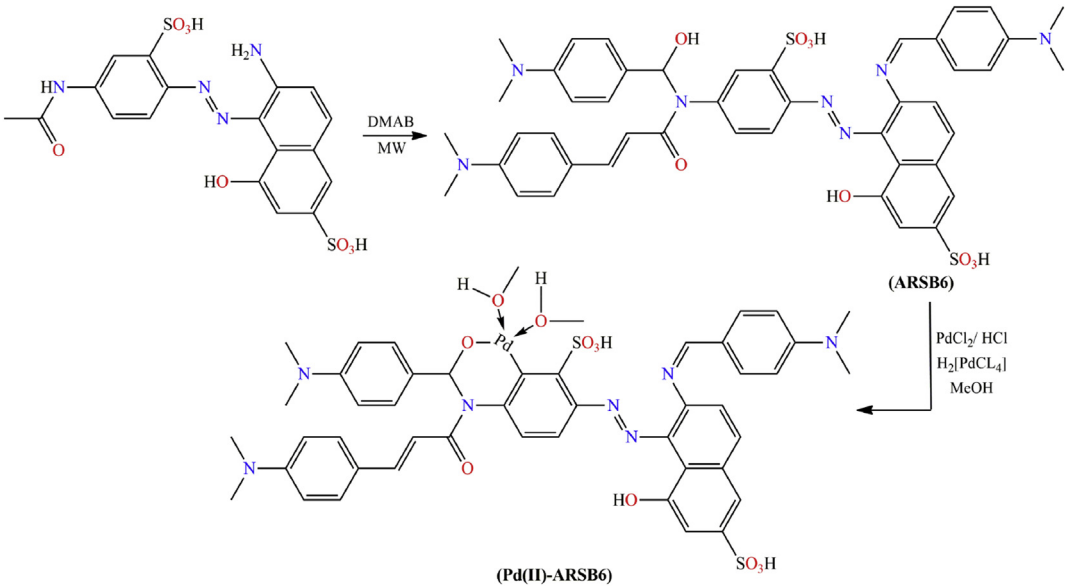

Scheme 3. Schematic preparation of ARSB**6** and its organopalladium complex.

participation of azo nitrogen and phenolic oxygen in the coordination sphere of Pd(II) ion belongs to these complexes. Moreover, consistent with the palladination of the phenyl segment of ARSB is the observation of a new medium stretch around 575 cm^{-1} assignable to C—Pd vibrational mode. In conclusion, FTIR data suggested that ARSB**1**—**3** architectures act as tridentate CNO-chelating ligands. On the other hand, the alcoholic-OH stretches, which have been observed in the FTIR spectra of the ARSB**4**—**6** around 2650 cm^{-1}, were missed from the spectra of their organopalladium complexes confirming the deprotonation of the alcoholic oxygen and replacement of alcoholic proton by Pd(II) ion. In addition, the infinitesimal changes in the position of the vibration band characteristics for azo (N=N) and phenolic (C—O) groups prove the departure of these moieties from the coordination sphere of Pd(II) ion. Finally, the broad band at ca. 3441—3401 cm^{-1} agrees with the hydrated nature of Pd(II)-ARSB**4**—**6** complexes as suggested by the microanalytical data. Conclusively, the ARSB**4**—**6** act as bidentate CO-chelating ligands.

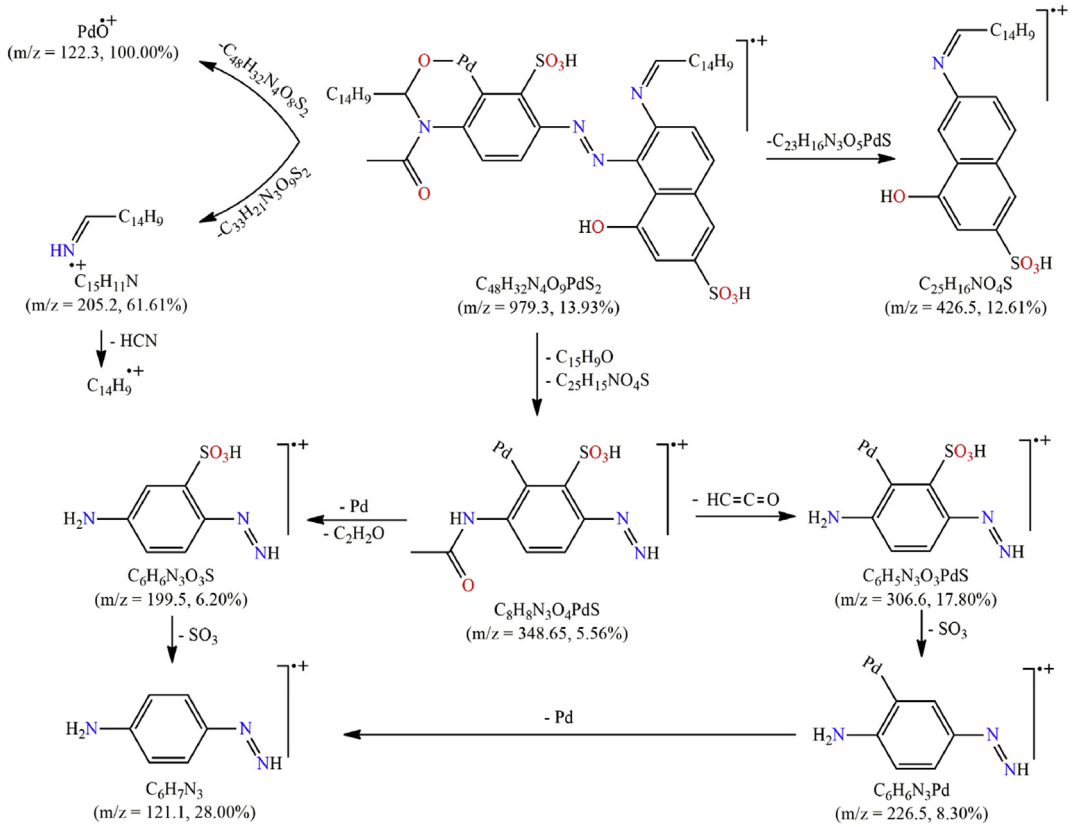

Scheme 4. All possible mass fragmentation pathways for (Pd(II)-ARSB**5**).

4.2.3. NMR studies

^{1}H NMR spectra of Pd(II)-ARSBs complexes are dominated by common remarkable features' evidence for their successful preparation: (1) the downfield shift of naphthyl-OH resonance for Pd(II)-ARSB**1**–**3** in comparison to parent ARSB**1**–**3**, by $\delta = +(0.08–0.15)$ ppm, corroborates the engaging of naphthyl-OH in coordination to Pd(II) ion. (2) The immutability of sulfonic (SO_3H), $\delta = 2.05 \pm 0.06$ ppm, and azomethine (H–C=N), $\delta = 8.10 \pm 0.15$ ppm, groups in the ^{1}H NMR spectra for all Pd(II)-ARSBs complexes as compared with native ligands suggested nonengagement of these moieties in chelation to Pd(II) ion. (3) The downfield shifts of phenyl-H resonances along with lowering of the proton integral value by one proton provide strong evidence replacement of such aromatic proton with Pd(II) ion (see Fig. 1).

4.3. Pharmacology

4.3.1. Antimicrobial activity

Parent ARSB ligands and Pd(II)-ARSB complexes were in vitro evaluated in comparison with standard antibiotics (antibacterial, Tetrcy; antifungal, Am B) for their efficacy to curb the growth of a common panel of pathogenic microbial species including *S. aureus* and *S. faecalis*, G^+ bacteria, *E. coli* and *P. aeruginosa*, G^- bacteria, and *A. flavus* and *C. albicans*, fungal pathogens. Generally, palladination of ARSBs synergistically enhanced the antibacterial and antifungal (i.e., antimicrobial) efficacies in comparison to the native ARSBs as revealed from the diameters of ZOI (Fig. 2). Also, noticeable, organopalladium complexes (and Pd(II)-ARSB**1**–**6**) exhibited a wide range of antibacterial activities from inactive derivative such as Pd-ARSB**3** to an extremely potent one Pd-ARSB**1** ($MIC_{E.\ coli/P.\ aeruginosa} = 1.18/2.65$ mM and $MIC_{S.\ aureus/S.\ faecalis} = 9.85/11.02$ mM). These promoted bactericidal activities of Pd(II) complexes can be explained on the basis of Overtone's concept [13] and Tweedy's chelation theory [14], which attributed the higher potency of complexes against pathogens to their enhanced liposolubility action owing to diminishing of the polarity of the Pd(II) ion through its coordination and partial sharing of its cationic charge with the donor sites of ARSBs. This enhanced lipophilicity facilitates penetration and diffusion of the target complex into the lipid membrane of pathogen along with blocking metal active enzymatic binding sites in the microorganisms.

Noteworthy, most tested compounds are less potent as fungicides where nearly all parent ARSBs are antifungal inactive except ARSB**4**, which exhibits moderate inhibitory activity against *A. flavus*, and a more potent antifungal agent, ARSB**5**, which has the ability to eradicate both fungal pathogens (*A. flavus* and *C. albicans*). However, organopalladium complexes demonstrated higher antifungal efficacy than the native ligands with significantly promoted antifungal activity registered for Pd-ARSB**1**. In conclusion, among assaying compounds, Pd-ARSB**1** was signed as the most potent and

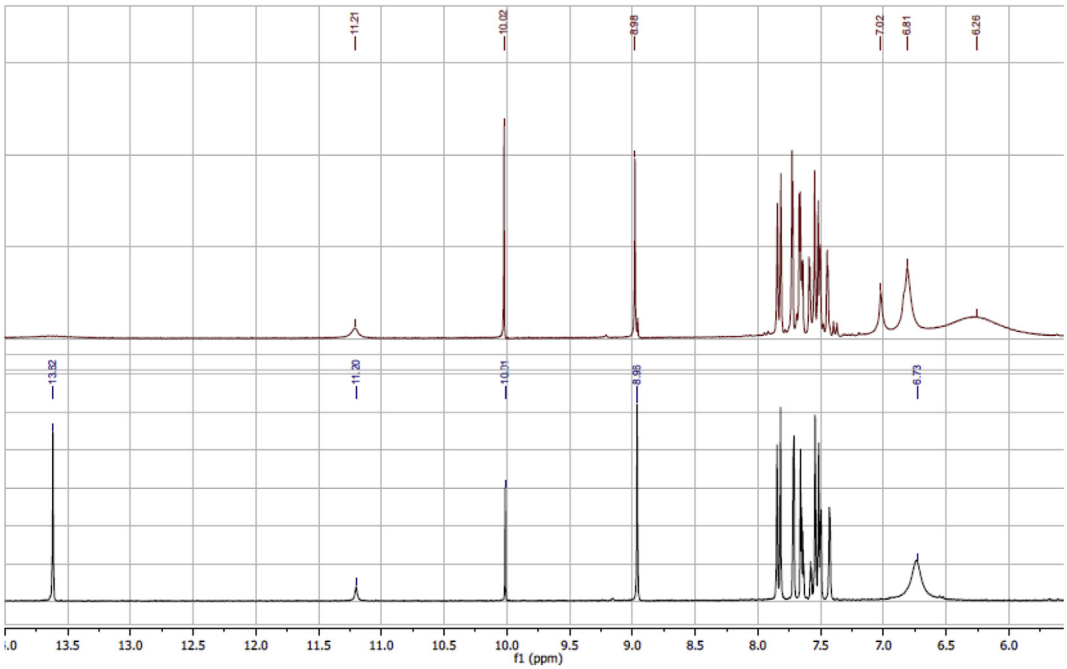

Fig. 1. Partial ^{1}H NMR region (6.0–14.0 ppm), for comparison of the phenolic protons' resonance and their splitting patterns in ARSB**4** and its Pd(II) complex.

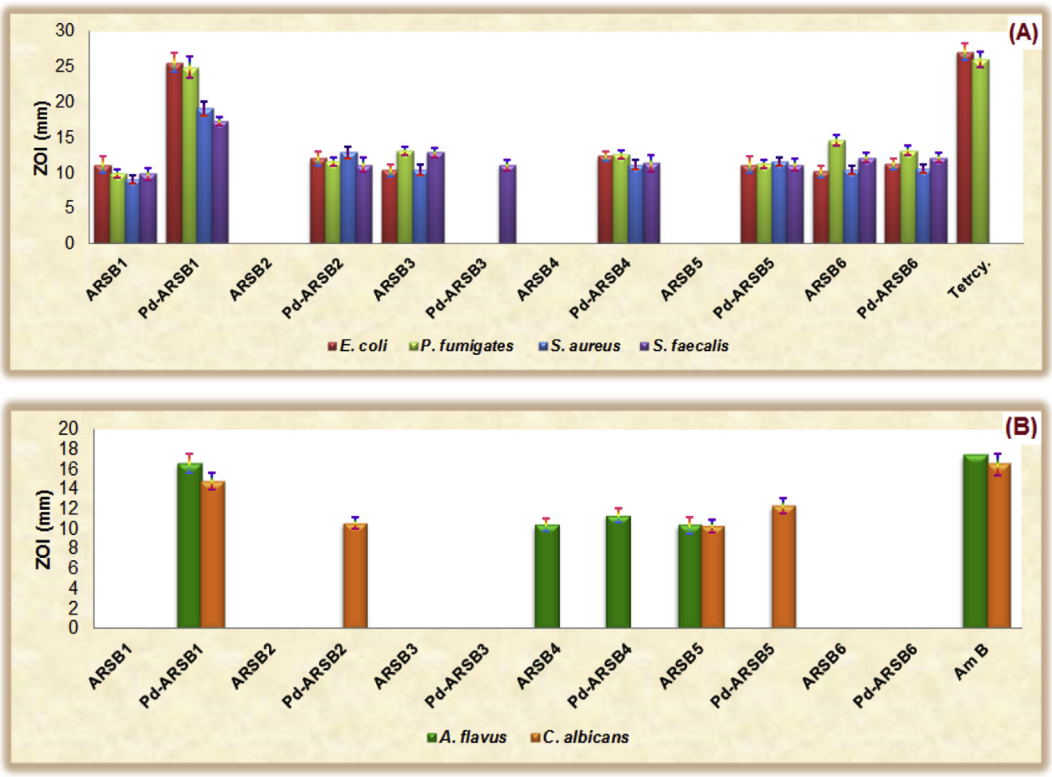

Fig. 2. Graph of zone of inhibition (ZOI, mm) for most ARSBs and their organopalladium complexes against (A) bacterial cells and (B) fungal strains.

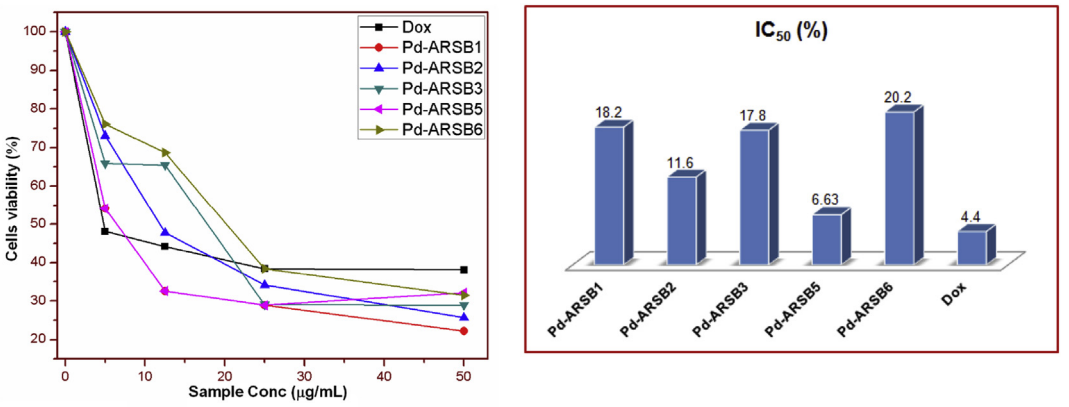

Fig. 3. Concentration-dependent antitumor efficacy assessment and IC_{50} values of new organopalladium complexes against human MCF-7 cell lines.

broad-spectrum antimicrobial agent ($MIC_{E.\ coli/P.\ aeruginosa}$ = 1.18/2.65 mM and $MIC_{S.\ aureus/S.\ faecalis}$ = 9.85/11.02 mM) and ($MIC_{A.\ flavus/C.\ albicans}$ = 12.50/14.10 mM). Inspired with this notice, further structural refinement along with intensive microbiological assessments for this organopalladium complex may open new avenue for generation of new promising antibiotic candidates.

4.3.2. Preliminary in vitro antitumor assay

Preliminary in vitro antitumor survey of new organopalladium complexes was investigated in comparison to a common antitumor drug, doxorubicin (Dox) ($C_{27}H_{29}NO_{11}$, 543.52 g/mol), against human breast carcinoma (MCF-7) cell lines. Noticeable, all selected complexes exhibit growth inhibitory effects against MCF-7 cell lines within structure –activity relationship profile as revealed from the depicted cell viability values in Fig. 3. Interestingly, refinement of the ARSB skeleton can modulate the anticancer efficacy of the organopalladium complex where the IC_{50} values for Pd-ARSB**5** and **6** are 6.63 and 20.2 μg/mL, respectively; consequently, Pd-ARSB**5** is a threefold more cytotoxic against MCF-7 cell lines than Pd-ARSB**6**. On the contrary, the Pd-ARSB**4** is fully inactive against MCF-7 cells. Memorably, the remarkable effectiveness of Pd-ARSB**5** as an MCF-7 antitumor agent in comparison to other organopalladium complexes could be attributed to the promoted non-polarizing effect of two anthranyl side groups, which significantly affected the DNA-organopalladium van der Waals interaction, whereas the hydrophobic nature of anthranyl segments enhances the van der Waals energy of Pd-ARSB**5**, causing an improvement in DNA-organopalladium association via van der Waals forces, which played a crucial role than hydrogen bonding in the binding of different anticancer agents to DNA [15].

5. Conclusions

Our protocol has succeeded in the conversion of harmful dye (AR-37) into new pharmacological candidates with synergistic antibacterial, antifungal, and anticancer performance. In this endeavor, the biocidal activities of the newly synthesized *endo*-cyclic five/six-membered cyclopalladated complexes (Pd(II)-ARSBs) have been investigated against common pathogenic G^+ and G^- bacterial and fungal strains. Moreover, the antitumor efficacy of these complexes against human breast carcinoma (MCF-7) cell lines has been addressed. The recorded ZOIs and MIC values revealed a moderate to superb broad-spectrum antimicrobial efficacy of cyclopalladated complexes (Pd(II)-ARSBs) in comparison to the parent ARSB standard antibiotic with a preferential efficacy to act as bactericides than fungicides. Structure –activity relationship for new organopalladium complexes against MCF-7 cell lines revealed a correlation between the hydrophobicity of the target compound, as tuned by the substituents, and its antitumor activity.

Appendix A. Supplementary data

Supplementary data related to this article can be found at http://dx.doi.org/10.1016/j.crci.2017.07.003.

References

[1] K. Selvam, K. Swaminathan, K.S. Chae, Bioresour. Technol. 88 (2) (2003) 115–119.
[2] S. Sharma, S. Sharma, P.K. Singh, R.C. Swami, K.P. Sharma, Bull. Environ. Contam. Toxicol. 83 (1) (2009) 29–34.
[3] P. Baldrian, J. Gabriel, FEMS Microbiol. Lett. 220 (2003) 235–240.
[4] I. Eichlerova, L. Homolka, F. Nerud, Bioresour. Technol. 97 (16) (2006) 2153–2159.
[5] (a) R.F.M. Elshaarawy, C. Janiak, Tetrahedron 70 (43) (2014) 8023–8032;
(b) R.F.M. Elshaarawy, Z.H. Kheiralla, A.A. Rushdy, C. Janiak, Inorg. Chim. Acta 421 (2014) 110–122;
(c) R.F.M. Elshaarawy, C. Janiak, Eur. J. Med. Chem. 75 (2014) 31–42.
[6] (a) R.F.M. Elshaarawy, I.M. Eldeen, E.M. Hassan, J. Mol. Struct. 1128 (2017) 162–173;
(b) R.F.M. Elshaarawy, T.B. Mostafa, A.A. Refaee, E.A. El-Sawi, RSC Adv. 5 (2015) 68260–68269;
(c) R.F.M. Elshaarawy, C. Janiak, Arab. J. Chem. 9 (2016) 825–834.
[7] P. Anand, V.M. Patil, V.K. Sharma, R.L. Khosa, N. Masand, Int. J. Drug Des. Dis. 3 (2012) 851–868.
[8] A.M. NASSAR, Met-Org. Nano-Met. Chem. 46 (2016) 1349–1366.
[9] M.A. Ali, A.H. Mirza, R.J. Butcher, M.T.H. Tarafder, T.B. Keat, A.M. Ali, J. Inorg. Biochem. 92 (2002) 141–148.
[10] E.A. El-Sawi, T.M. Sayed, H. Khalifa, Int. J. Curr. Res. Aca. Rev. 2 (2) (2014) 35–47.
[11] C. Perez, P. Bazerque, Acta Biol. Med. Exp. 15 (1990) 113–115.
[12] T. Mosmann, J. Immunol. Methods 65 (1983) 55–63.
[13] N. Dharamaraj, P. Viswanathamurthi, K. Natarajan, Transit. Met. Chem. 26 (2001) 105–109.
[14] R. Malhota, S. Kumar, K.S. Dhindsa, Indian J. Chem. 32A (1993) 457–459.
[15] I. Ali, W.A. Wani, K. Saleem, M.-F. Hsieh, RSC Adv. 4 (2014) 29629–29641.